Homeostatic swimming of zooplankton upon crowding: the case of the copepod *Centropages typicus*

Marco Uttieri,[1,2,*] Peter Hinow,[3,†] Raffaele Pastore,[4,‡] Giuseppe Bianco,[5] Maurizio Ribera d'Alcalá,[1] and Maria Grazia Mazzocchi[1]

[1]*Department of Integrative Marine Ecology, Stazione Zoologica Anton Dohrn, Villa Comunale, 80121 Naples, Italy*

[2]*CoNISMa, ULR Partehnope, Piazzale Flaminio 9, 00196 Rome, Italy*

[3]*Department of Mathematical Sciences, University of Wisconsin - Milwaukee, Milwaukee, WI 53201, USA*

[4]*Department of Chemical, Materials and Production Engineering, University of Naples Federico II, P.le Tecchio 80, Napoli 80125, Italy*

[5]*Department of Biology, Lund University, Sölvegatan 37, 22362 Lund, Sweden*

Crowding has a major impact on the dynamics of many material and biological systems, inducing effects as diverse as glassy dynamics and swarming. While this issue has been deeply investigated for a variety of living organisms, more research on the effect of crowding on the behaviour of copepods, the most abundant metazoans on Earth, remains to be done. We experimentally investigate the swimming behaviour, used as a dynamic proxy of animal adaptations, of males and females of the calanoid copepod *Centropages typicus* at different densities of individ-

uals (10, 50 and 100 ind. L^{-1}) by performing three-dimensional single-organism tracking. We find that the *C. typicus* motion is surprisingly unaffected by crowding over the investigated density range. Indeed, the mean square displacements as a function of time always show a crossover from ballistic to Fickian regime, with poor variations of the diffusion constant on increasing the density. Close to the crossover, the displacement distributions display exponential tails with a nearly density-independent decay length. The trajectory fractal dimension, $D_{3D} \cong 1.5$, and the recently proposed 'ecological temperature' also remain stable on increasing the individual density. This suggests that, at least over the range of animal densities used, crowding does not impact on the characteristics of *C. typicus* swimming motion, and that an homeostatic mechanism preserves the stability of its swimming performance.

Keywords: *Centropages typicus*; crowding; random walk; fractal dimension; mean square displacement; ecological temperature

1. INTRODUCTION

Crowding dramatically affects the dynamics of a wide variety of material and living systems, from colloidal suspensions to animal assemblies. Crowding leads, indeed, to complex effects, even in systems as simple as Brownian hard-sphere suspensions [1], where the dynamics is uniquely determined by

* marco.uttieri@szn.it

† hinow@uwm.edu

‡ raffaele.pastore@unina.it

the excluded volume and the entropy. On increasing the volume fraction in a narrow range, in fact, particle motion becomes sluggish and develops long-range correlations [1], up to a structural arrest. Such a "glassy" slow-down on crowding also characterizes complex fluids and a variety of living and active systems, including microswimmers, cells and ants [2–4]. However, antagonistic dynamics may also be at play upon crowding. For example, swarming is a spectacular collective effect preventing the slow-down in crowded conditions for animals capable of coordinated response [5, 6].

Little is known, however, about the effect of crowding on copepods, the most abundant metazoans on Earth [7]. These crustaceans play a key role in the functioning of aquatic ecosystems, sustaining the vertical fluxes of matter and energy and linking lower and higher trophic levels [8]. In natural conditions, copepod density is in the range of few individuals per liter. However, copepods can also occur in dense aggregations with densities $> 10^3 - 10^4$ ind. L^{-1} [9–11]. Similar values can be reached also in artificial conditions when a large number of individuals is needed for experimental trials [12], for aquaculture purposes [13–15] or when recording the motion of copepods [16]. As a drawback, high densities may impair copepod fitness, reducing food availability and egg production whilst increasing mortality [17–19], boosting the concentration of metabolic products and reducing water quality [20] and decreasing the respiration rate [15]. In addition, increasing copepod abundance can favour the transfer of oil droplets to lower trophic level by direct manipulation and egestion [21]. These arguments emphasise the importance of improving current knowledge about the effects of crowding on the fitness of these tiny crustaceans.

The calanoid copepod *Centropages typicus* Krøyer, 1849 is a temperate Atlantic species widespread in coastal and neritic waters over a wide latitudinal range, including the adjacent Mediterranean Sea, where it is abundant espe-

cially in the Western Basin [22]. It is one of the best know copepod species (*approx.* 1.5 mm total body length in box adult sexes), thanks to extensive studies investigating its ecology, biology and behaviour [23, 24]. In the present contribution we investigate the potential effects of different population densities on the swimming performance of this species. In copepods, changes in motion patterns as a result of endogenous and/or exogenous stresses may affect the search for food and mates, as well as the escape from predators [25, 26]. Alterations in motion features can also be employed to assess, on short temporal scales, sublethal behavioural endpoints [27]. The goal of this study is to evaluate if and to which extent does crowding alter the characteristics of *C. typicus* swimming motion, and consequently the overall fitness of this species. To address this topic, we carried out an integrated analysis by combining multiple descriptors to gather a detailed characterization of the 3D *C. typicus* swimming behaviour under different population densities. First, length and time scales characterizing *C. typicus* motion are quantified through the mean square displacement and the displacement distributions [28]. Next, the fractal dimension of the trajectories is estimated [29, 30] in order to probe their degree of space-occupancy. Finally, the ecological temperature [31] is exploited to evaluate the activity level of *C. typicus* under different crowding levels. The integration of these indicators leads to join the macroscopic (ensemble averaged) properties of the system to the microscopic (single-organism) behaviour of its components.

2. METHODS

2.1. Experimental design

Individuals of *Centropages typicus* were collected at the coastal station LTER-MC (40.8080° N; 14.2500° E) in the Gulf of Naples (Tyrrhenian Sea, Western Mediterranean Sea), where this species is abundant and shows a clear seasonal cycle with regular peaks in late spring-early summer [32, 33]. It is one of the most abundant copepod species at LTER-MC, where it accounts for an annual mean of 6.8 ± 2.5 % of the total and very diversified copepod assemblage, and reaches peak concentrations of 2.4 ind. L^{-1} [32].

Zooplankton samples were collected in spring 2008 through gentle vertical tows in the upper 50 m of the water column using a Nansen net (200 μm mesh size) mounting a 5 L non-filtering cod end. In the laboratory, the sample was diluted and *C. typicus* individuals were manually sorted with a large-bore glass pipette and checked for stage, sex and overall integrity under an Olympus SZH10 dissecting microscope. Only undamaged and healthy adult males and females were kept for the subsequent video recordings.

Freely swimming individuals were recorded using a 3D system, equipped with two orthogonal digital CCD cameras (Sony XCD-X700, operating at 15 fps) mounting custom telecentric lenses; the filming was carried out in absence of visible light, using only two background LED infrared panels (780 nm, 18 mW) (see [34]). The system guaranteed a spatial resolution of 78 μm, sufficient to discriminate between single individuals. The cameras overlooked an experimental volume of $80 \times 80 \times 60$ mm (384 mL), representing a fraction (~ 38%) of the entire aquarium (1 L) where the animals could swim freely without any wall effect. Apart from the small volume, the experimental conditions were similar to the environment of *C. typicus*. The aquarium was filled with sea water sampled *in situ*, enriched with 7.0×10^3 microzooplankton cells L^{-1} and

1.5×10^7 phytoplankton cells L^{-1}. All experiments were carried out at 17 °C, reproducing environmental temperature.

Three different copepod densities were tested, namely 10, 50 and 100 ind. L^{-1}. These values were 4 to 42 times higher than the highest *C. typicus* abundance *in situ* [32]. The first value tested (10 ind. L^{-1}) is in the range of densities used in the literature in copepod behavioural studies [16]. Such densities increase the probability of recording a sufficient number of tracks, while at the same time leaving enough free space to the individuals to move independently of the others [16]. The other two values, 50 and 100 ind. L^{-1}, were instead selected to test the effect of increasing densities on the individual behaviour. Each sex was recorded separately to avoid any mate-seeking behaviour. Copepods were acclimated for a minimum of 15 min before recording. The acclimatization was done each time a new group of individuals was added to increase the density.

Once recorded, the tracks described by single individuals were digitized using a custom software [34], providing the (x, y, z) coordinates at each time step t. The length of the tracks varied, depending on the time each copepod was in focus in the arena. For the evaluation of the fractal dimension and for the calculation of the ecological temperature, only tracks lasting approximately 60 s were considered. Such threshold was necessary to ensure a statistically meaningful time span to characterize the tracks efficiently. For the calculation of the mean squared displacement and the displacement distributions, a wider data set was instead used, including all tracks lasting more than 5 s.

2.2. Characterization of *C. typicus* swimming behaviour

The 3D tracks digitised were numerically characterised by integrating different descriptors, each focusing on a specific aspect of *C. typicus* motion. In the

following we illustrate briefly the parameters used; a more detailed description is given in the Supplementary Materials.

The mean square displacement (MSD) and the associated distribution of displacements *C. typicus* were calculated over several decades in time, length and probability. These descriptors have been used in different fields of investigation, including zooplankton behaviour [28, 35]. The MSD represents the average square distance $\langle \Delta r^2(\Delta t) \rangle$ covered by an individual over a time interval Δt, whereas the displacement distribution $G_s(l, \Delta t)$ is the probability density that an individual has moved a distance l over the time Δt. These metrics were measured both on the 3D tracks, as well as separately on the horizontal plane $((x, y))$ and vertical direction (z) to distinguish any possible effect induced by gravity. Since there are no relevant differences, we find it more concise and instructive to focus only on the 3D case. These descriptors allow discriminating between standard (Fickian) and anomalous (ballistic) diffusion in *C. typicus* motion [36] (see also Sec.1.1 of Supplementary Material).

Zooplankton tracks have been robustly described in terms of their fractal properties [30]. The fractal dimension D provides an estimate of the space-filling tendency of an object. In this work, the three-dimensional (3D) fractal dimension D_{3D} of *C. typicus* tracks was estimated to discern any possible behavioural change induced by crowding, using the protocol described in [29]. D_{3D} was also used to compare the motion of males and females exposed to the same density of organisms. The fractal dimension was also estimated on the 2D projections of the tracks (D_{xy}, D_{xz} and D_{yz}) to evaluate any possible anisotropy in the motion.D_{3D}, D_{xy}, D_{xz} and D_{yz} values were statistically analysed to ascertain any significant difference among the groups. The groups were compared using a non-parametric Kruskal-Wallis H test, if necessary complemented with a *post hoc* multiple pairwise comparison with Dunn-Šidák's correction. The accuracy in the estimations was assessed through the coefficient of determination

(R^2) of the regression lines and the root mean square error (RMSE).

The notion of ecological temperature is inspired by the Maxwell-Boltzmann kinetic theory [31] and follows earlier ideas in [37]. The mean square speed v^2 of individual *C. typicus* was employed to define a "single-organism temperature" accounting for individual activity, considering that single specimens may modify their motion activity as a function of physiological triggers. The cumulative distribution functions of the individual ecological temperatures was then used to evaluate differences in motion behaviour associated with crowding conditions experienced by *C. typicus*. The Kolmogorov-Smirnov test was used to distinguish pairs of empirical cumulative distributions.

3. RESULTS

The behaviour of *Centropages typicus* (Figure 1) is characterised by three motion states namely swimming, sinking and jumping. In the typical swimming habit, the body of *C. typicus* females and males is slightly oblique, describing an helical path. At variable frequency, the copepods alternate such behaviour to sinking, *i.e.* a passive downward displacement without any movement of the cephalothoracic appendages. Only rarely *C. typicus* females and males display quick (< 0.1 s) and long (> 10 mm) jumps.

3.1. Mean square displacement

Figure 2 (a) shows the 3D MSD as a function of time for all recorded experiments. We use a bi-logarithmic plot to have a clear overview of the motion over the different investigated time scales. On this scale, the absence of a clear-cut trend upon changing the concentration, or sharp differences between females and males, is clearly noticeable. Conversely, a common behaviour emerges

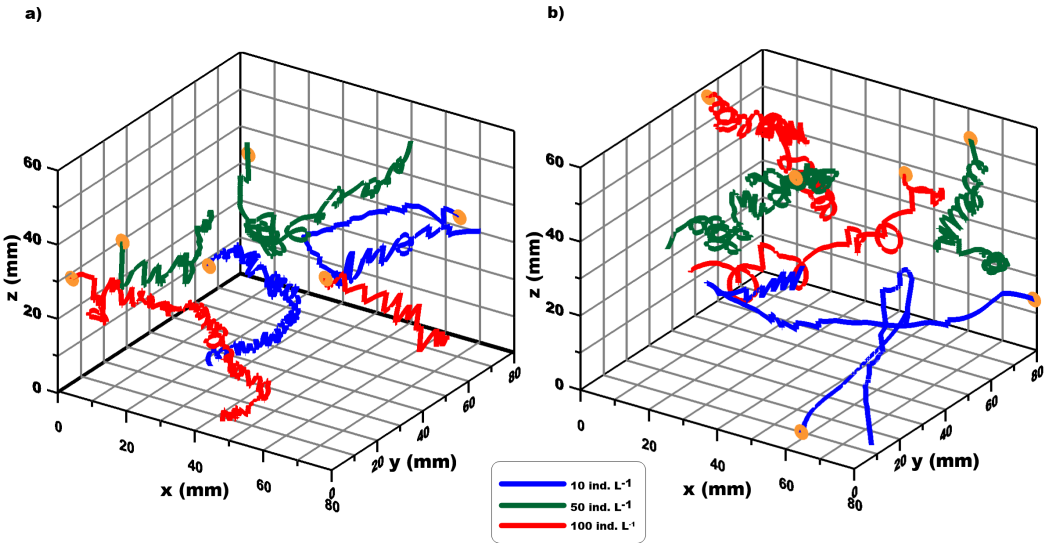

FIG. 1. Representative 3D trajectories of freely swimming *Centropages typicus* females (a) and males (b) at the experimental concentrations of 10 (blue), 50 (green) and 100 (red) ind. L^{-1}. For each condition and sex, the trajectories of two randomly chosen individuals are plotted. The starting point of each track is marked with an orange circle. The trajectories are plotted in an isometric reference frame resembling the observation window of the experimental setup.

from all datasets investigated. At short times, $\Delta t \leq 1$ s, the MSD increase is compatible with ballistic diffusion, $\langle \Delta r^2(\Delta t) \rangle \propto \Delta t^2$. At intermediate time, $\Delta t > 1$ s, a smooth crossover takes place, where the MSDs slow down toward a Fickian regime, $\langle \Delta r^2(\Delta t) \rangle = 6 D_L \Delta t$, with D_L being the long-time diffusion coefficient. Fickian diffusion is in fact attained at times close to the overall observation time, $\Delta t \simeq 10$ s. Overall, *C. typicus* females and males perform straight and sudden steps at short times (on the timescale of the ballistic regime) and subsequent steps are poorly correlated, giving rise to a random-walk-like motion on longer timescales (corresponding to the Fickian regime).

To get more details on changes induced by individual density and sex, Figure 2b shows the same data as Figure 2a in linear scale. This implies that we are now focusing only on the last decade in time ($\simeq 1 - 30$ s), corresponding to the Fickian regime. Within this visualization, some spreading among different

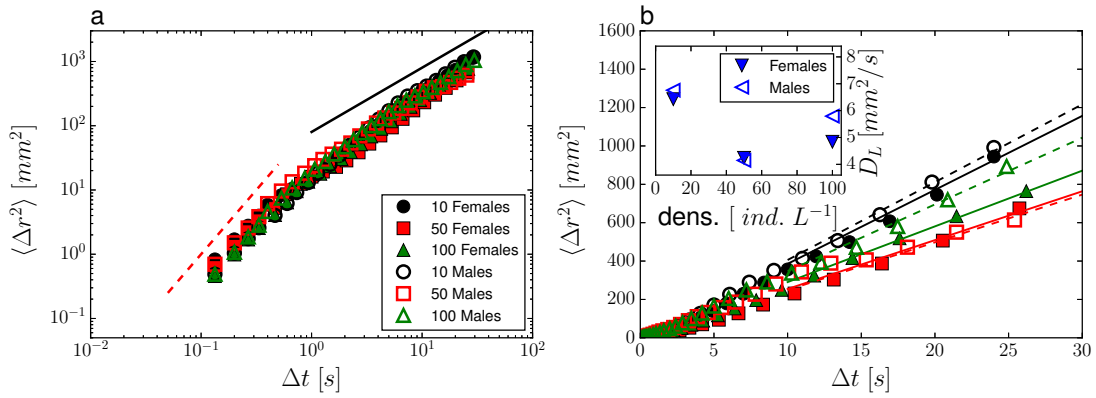

FIG. 2. (a) Bi-logarithmic and (b) linear plot of MSD as a function of time for females (full symbols) and males (empty symbols), at different individual densities, as indicated. The lines in panel a are guides to the eyes, indicative of ballistic diffusion (dashed), $\langle \Delta r^2(\Delta t) \rangle \propto t^2$, and Fickian diffusion (solid), $\langle \Delta r^2(\Delta t) \rangle \propto \Delta t$, respectively. The lines in panel b are long-time fits $\langle \Delta r^2(\Delta t) \rangle = 6 D_L \Delta t$ for females (solid) and males (dashed), with the diffusion coefficient D_L being the fitting parameter. Inset: D_L as a function of the individual density for both females (full symbols) and males (empty symbols). The symbol size is similar to the errors on D_L, as obtained from the fits.

datasets is detectable. In order to readily capture this variation, we measured the diffusion coefficient D_L, through a long-time Fickian fit to the data. The obtained estimation of D_L is shown in the inset of Figure 2b as a function of the individual density, for both females and males. The diffusion coefficient lies in the range $4 - 7$ mm^{2}s^{-1} and does not show a clear, monotonic trend at increasing densities. Conversely, data for both females and males display a moderate minimum at the intermediate investigated density of 50 ind. L^{-1} a factor of about 0.75 smaller than the average diffusion coefficient. This result calls for future experimental campaigns to sample the intermediate density range through many other experiments, so as to clarify whether the observed minimum originates from a smooth trend or simply from statistical noise. We also notice that at the highest density, *i.e.* 100 ind. L^{-1}, the male diffusion coefficient is is a factor of about 1.2 larger than the female one. This suggests that, on average, males move faster than females, consistently with a previous experiments

that also measured the diffusion coefficient for the same species [38].

With regards to the spatial isotropy of the motion, the results drawn for the three-dimensional MSD are found to be qualitatively similar to those obtained analysing the horizontal and vertical components separately.

3.2 Distribution of individual displacements

Figure 3 provides a broad overview of the distribution of organism displacements, $G_s(l, \Delta t)$. The three panels refer to the different investigated crowding conditions and report $G_s(l, \Delta t)$ both for males and females. The selected time Δt falls within the ballistic regime ($\Delta t = 0.67$ s), the ballistic-Fickian crossover ($\Delta t = 2$ s), and the Fickian regime ($\Delta t = 10$ s), respectively. A distinctive feature emerging from Figure 3 is the clear evidence of fat (*i.e.*, fatter than Gaussian), exponential-like tails at the intermediate time.

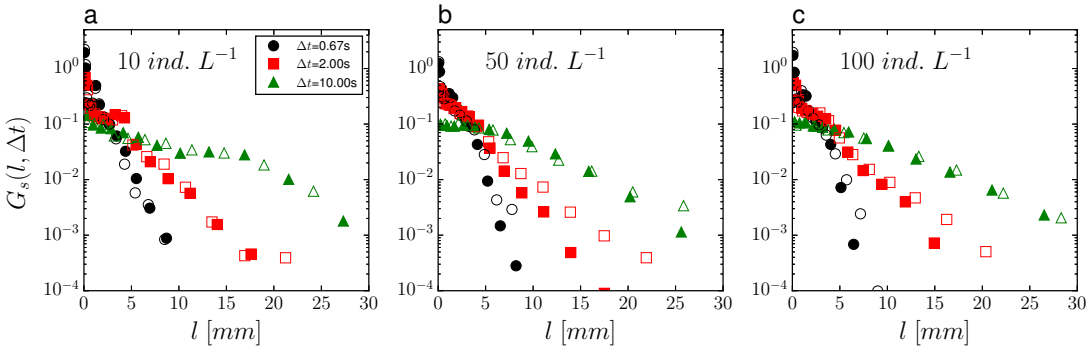

FIG. 3. Displacement distribution, $G_s(l, \Delta t)$ of females (full symbols) and males (empty symbols) as function of the displacement length l, and at different times Δt, as indicated. The individual density is 10, 50 and 100 ind. L^{-1} in panel a, b and c, respectively.

At shorter time, the distribution is instead more similar to a Gaussian. A hint to restore the Gaussian property seems to be present also at the longest time in Figure 3, as expected for a standard random walk. Overall, Figure 3 confirms

that no major differences exist between the groups of males and females. Slight deviations in the tails are observed only at the intermediate time $\Delta t = 2s$, and densities 50 and 100 ind L^{-1}, where the characteristic decay length of males is a factor about 1.75 and 1.3, respectively, larger than the female one (as obtained through exponential fits).

To better observe this aspect as well as the exponential nature of the tails at intermediate time, Figure 4 shows a direct comparison between the distribution at the different densities and a time $\Delta t = 1$ s, corresponding to the overall duration ballistic regime (*i.e.*, right at the edge between ballistic regime and ballistic-Fickian crossover). By doing so, the distributions of single ballistic steps are monitored. Accordingly, the exponential tails appearing in Figure 4 reveal the heterogeneous distribution of these steps. Remarkably, datasets corresponding to different densities nearly overlap both for females (panel a) and males (panel b), indicating that the decay length is essentially constant at different crowding conditions.

Concerning the spatial isotropy of the displacement distribution, the only noticeable difference is a local maximum in $G_s(l, \Delta t)$ at short time ($\Delta t = 0.67s, 1s$ and $2s$ in Fig.s 3 and 4) and relatively small lengths (*e.g.*, $\simeq 2.5$ mm in fig.4), which is clearly detectable in three dimensions, but absent in the distribution of the horizontal displacements. This local maximum is readily ascribed to the gravity-induced drift in the vertical direction. As time progresses, such a passive displacement is progressively overwhelmed by the "active" motion, with the consequent disappearing of the local maximum.

3.3 Fractal dimensions of swimming tracks

The characterisation of the tracks in terms of their D_{3D} reveals several intriguing aspects of the motion behaviour of *C. typicus*. All tracks display an

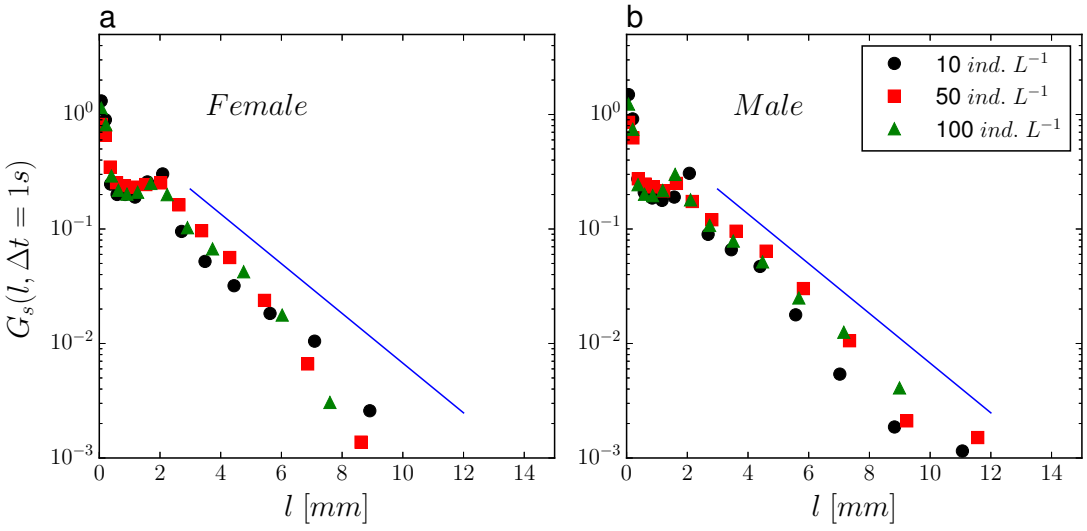

FIG. 4. The displacement distribution $G_s(l, \Delta t)$ for females (a) and males (b), as function of the displacement length l, at an intermediate time $\Delta t = 1$ s, and for the indicated densities. The solid lines are guides to the eyes, indicative of an exponential decay, $G_s(l, \Delta t) \propto e^{-l/\xi}$, with $\xi = 2$ mm.

intermittent and recursive alternation in the magnitude of the instantaneous 3D displacements at different temporal scales, which constitutes an underlining signature of a fractal process (not shown). As evident from Figure 5, both females and males describe moderately convoluted tracks, with mean D_{3D} values between 1.15 and 1.21 (Table I). Remarkably, this range of values falls in between the fractal dimensions of ballistic motion and random walk (1 and 2, respectively), consistent with the MSD results; consequently the estimated D_{3D} can be considered as characteristic of a mixed, ballistic/random-walk-like motion. The non parametric Kruskal-Wallis analysis of variance results in p = 0.64, indicating overall statistical similarity among the D_{3D} recorded both by each sex in the three different conditions, and by females and males at the same level of crowding, as further confirmed by the boxplots (Figure 5). The R^2 and RMSE returned values close to one and zero, respectively, in all D_{3D} estimates

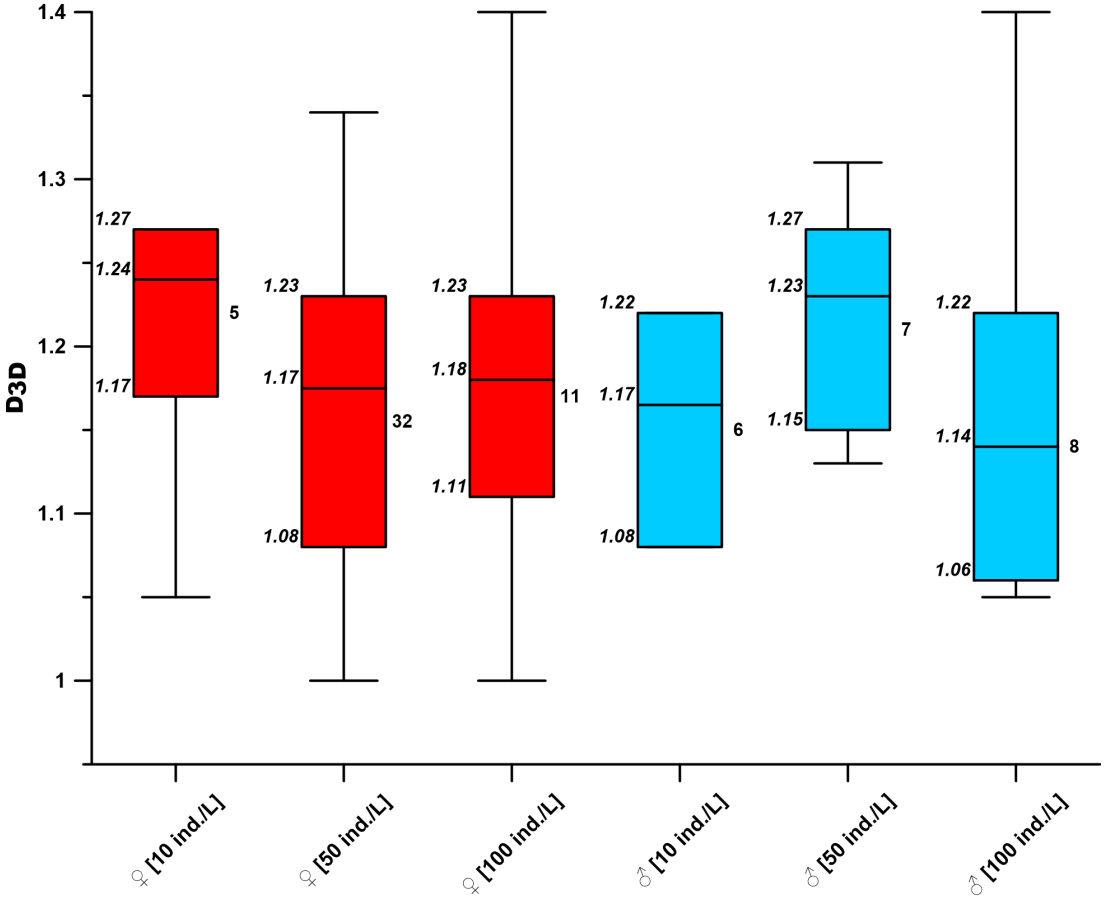

FIG. 5. Boxplots of the D_{3D} values for *Centropages typicus* females (red) and males (sky bule) under the different crowding conditions analysed. On the right of each box the number of samples for each group is reported, while on the left the 25^{th}, 50^{th} and 75^{th} percentiles are indicated.

(Table I), thus ensuring robustness of the method.

In 2D, for each crowding condition, the D_{xy}, D_{xz} and D_{yz} of a given sex are always statistically similar (Kruskal-Wallis analysis of variance $p > 0.01$) (Table II). This indicates that both females and males move isotropically in their environment. This outcome is backed up by the analysis of the boxplots (not shown). The confidence in the fractal dimension estimations is ensured by R^2 close to 1 and by low RMSE values (Table II). Additionally, the analysis of the interquartile ranges from the boxplots points to a comparable inter-

individual variability in the fractal dimension, thus mirroring crowding unbiased behaviour in both sexes.

Crowding Condition	D_{3D}	R^2	RMSE
♀ 10 ind. L^{-1}	1.20 ± 0.09	0.98 ± 0.02	0.13 ± 0.06
♀ 50 ind. L^{-1}	1.17 ± 0.09	0.97 ± 0.02	0.16 ± 0.05
♀ 100 ind. L^{-1}	1.18 ± 0.10	0.98 ± 0.01	0.12 ± 0.05
♂ 10 ind. L^{-1}	1.15 ± 0.07	0.98 ± 0.01	0.13 ± 0.04
♂ 50 ind. L^{-1}	1.21 ± 0.07	0.96 ± 0.02	0.18 ± 0.03
♂ 100 ind. L^{-1}	1.16 ± 0.10	0.97 ± 0.01	0.15 ± 0.04

TABLE I. D_{3D}, R^2 and RMSE values for *Centropages typicus* females and males under the different crowding conditions tested. All values were statistically similar.

3.4 Ecological temperature

The cumulative distribution functions of the ecological temperature are shown in Figure 6 and in Figure S1. The Kolmogorov-Smirnov test leads to the rejection of the null hypothesis that the data are drawn from the same distribution in all cases (Table SI). The deviation from the overall behavior shown by the males at their lowest density is within the range of variability of the ecological temperature among the treatments. As a matter of fact, the average ecological temperatures of the different experiments is constant within the standard deviation (Figure 7). For each density, the comparison between the genders is Figure S1.

4. DISCUSSION

Investigating the modalities by which individual organisms integrate exogenous information from their environment as well endogenous stimuli, and use

Crowding Condition	xy	xz	yz	Parameter
♀ 10 ind. L^{-1}	1.11 ± 0.07	1.20 ± 0.09	1.21 ± 0.08	D_{2D}
	0.99 ± 0.01	0.99 ± 0.01	0.99 ± 0.01	R^2
	0.09 ± 0.02	0.09 ± 0.03	0.09 ± 0.03	$RMSE$
♀ 50 ind. L^{-1}	1.18 ± 0.12	1.25 ± 0.13	1.26 ± 0.12	D_{2D}
	0.98 ± 0.01	0.99 ± 0.01	0.99 ± 0.01	R^2
	0.12 ± 0.04	0.11 ± 0.03	0.11 ± 0.03	$RMSE$
♀ 100 ind. L^{-1}	1.15 ± 0.11	1.23 ± 0.08	1.24 ± 0.12	D_{2D}
	0.99 ± 0.01	0.99 ± 0.01	0.99 ± 0.01	R^2
	0.09 ± 0.04	0.09 ± 0.02	0.10 ± 0.03	$RMSE$
♂ 10 ind. L^{-1}	1.11 ± 0.07	1.22 ± 0.07	1.23 ± 0.09	D_{2D}
	0.99 ± 0.01	0.99 ± 0.07	0.99 ± 0.01	R^2
	0.10 ± 0.03	0.10 ± 0.03	0.09 ± 0.02	$RMSE$
♂ 50 ind. L^{-1}	1.27 ± 0.11	1.27 ± 0.10	1.30 ± 0.11	D_{2D}
	0.98 ± 0.01	0.99 ± 0.01	0.98 ± 0.01	R^2
	0.12 ± 0.03	0.11 ± 0.02	0.13 ± 0.03	$RMSE$
♂ 100 ind. L^{-1}	1.16 ± 0.14	1.21 ± 0.10	1.24 ± 0.11	D_{2D}
	0.98 ± 0.01	0.99 ± 0.01	0.98 ± 0.01	R^2
	0.11 ± 0.03	0.10 ± 0.02	0.11 ± 0.03	$RMSE$

TABLE II. Isotropic fractal behaviour of *Centropages typicus* females and males. For each crowding condition and two-dimensional projection (xy, xz and yz planes), the values for D_{2D}, R^2 and RMSE are reported. All values were statistically similar.

them accordingly to modulate their behaviour, is central to relate movement ecology to community theory and biodiversity research [39]. Individual movement in animal kingdom displays a wide gamut of patterns and typologies [40, 41] . It can be modulated by triggers working at individual, population, community or ecosystem levels, and in a feedback loop variations in movement can impact on each of these hierarchically organised levels of aggregation [40]. Animal movement is generally quantitatively characterized by analysing the trajectory patterns [40, 42]. Such quantification permits the comparison of different behaviour and the emergence of peculiar strategies or adaptations to

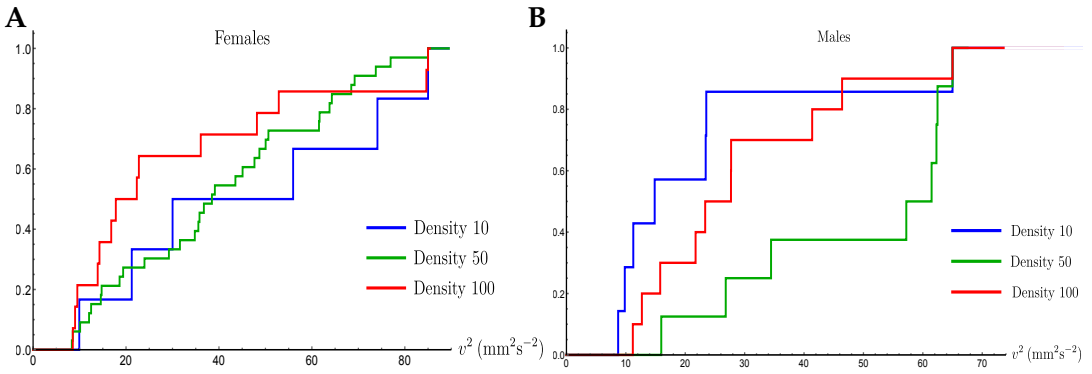

FIG. 6. Cumulative distribution functions of ecological temperature of ensembles of *C. typicus* females (**A**) and males (**B**) at different densities.

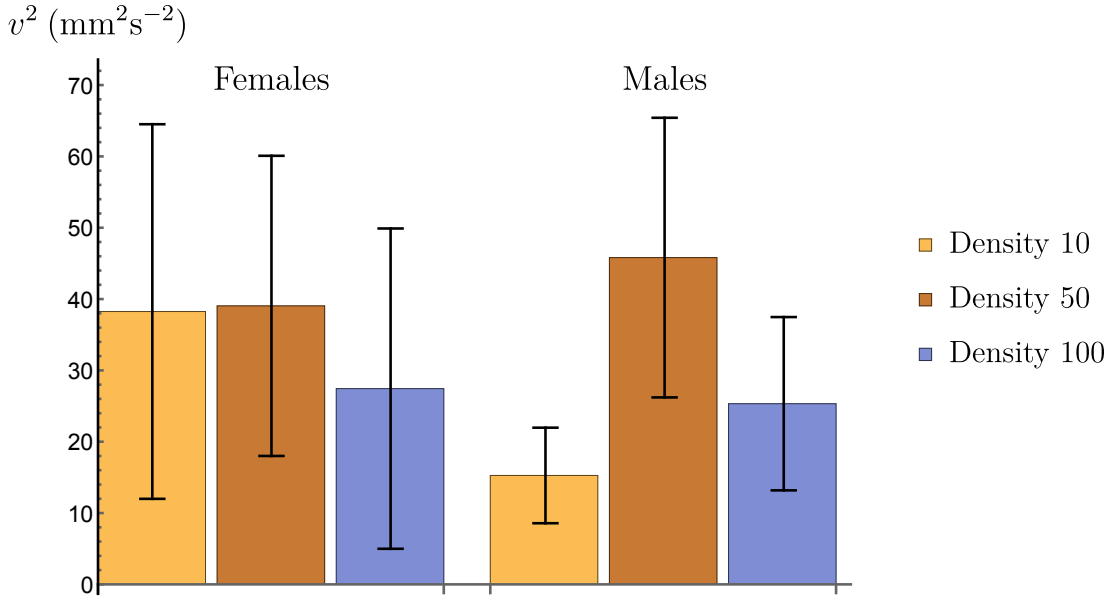

FIG. 7. The averages and standard deviations of the ecological temperatures for both sexes.

specific conditions. The results in the present study reveal new features of the behavioural adaptations of *Centropages typicus*, a planktonic copepod common in tropical to temperate waters of the Northern hemisphere. Adult females and males were exposed to three crowding conditions (10, 50 and 100 ind. L^{-1}), and their swimming trajectories were analysed in terms of mean square dis-

placement, displacement distributions fractal dimension and ecological temperature.

Behavior can hint at possible stress in organisms that may impact on their physiological state [43]; consequently a change in one of these parameters may reflect a change in the others. The complexity in spatial and temporal patterns of *C. typicus* swimming motion can therefore be used as a proxy of behavioural stress [27, 44], unveiling important underpinning biological and ecological responses. The integrated outcome emerging from the application of the above listed descriptors excludes any appreciable effect of crowding on the behavioural metrics tested. Inter-individual variations in movement can be linked to peculiar traits in the species investigated [40]. Independently of the treatment considered, both *C. typicus* females and males manifest coherent motion patterns, indicative of negligible inter-individual changes. This suggests that the responses recorded in this study do not depend on the internal state of the single individuals, but rather can be considered as population-level adaptations.

4.1. Homeostatic mechanisms

The scenario emerging from our results suggests that an homeostatic mechanism may be at play, preserving the swimming performance typical of dilute conditions in spite of the increasing individual density. Here we adopt the term homeostatic as commonly used in a broad context - including generic models of dynamical systems [45], brain plasticity [46], artificial intelligence [47], networks [48] - to indicate a category of dynamical processes where a system continuously self-organizes in order to maintain a targeted stationary condition.

Indeed, a simple possibility to understand our results is that the organisms tend to avoid clustering and dynamically maintain a spatial distribution that

closely maximizes their average distance λ, making the effect of crowding negligible, at least over the investigated density range. Indeed, maximizing λ closely corresponds to minimize the encounter rate, the local food consumption and, of course, any other type of interaction among different organism. As a matter of fact, homogeneous spatial distributions of individuals do maximize the average inter-organism distance.

It is therefore interesting to compare the values of l for spatially homogeneous distributions at the different densities with the characteristic length-scales that can be identified from the MSD. Assuming a spatially homogeneous distribution of individuals, the average distance among nearest neighbours is given by $\lambda = \left(\frac{V}{N}\right)^{1/3}$. This corresponds to $\lambda = 46.4, 27.1, 21.5\ mm$ for the experiments at densities 10, 50, 100 ind. L^{-1}, respectively. On the other hand, the typical, closely density-independent length of the ballistic step is $\xi_b \simeq 4mm$, as estimated by evaluating $\langle \Delta r^2(\Delta t) \rangle^{1/2}$ at the end of the ballistic behaviour $\Delta t = 1s$. Similarly, the root MSD at $\Delta t = 25s$, a time-span corresponding to the typical trajectories duration, provides an estimation of the overall distance, ξ_{max}, travelled by an organism during the whole observation time. For instance, $\xi_{max} \simeq 28mm$, at the highest density. Accordingly, the average inter-organism distance λ is always significantly larger than the ballistic step and comparable with the overall travelled distance, even at the largest individual density.

Further exploiting this framework, it is possible to evaluate the timescales, τ_o, on which the regions explored by nearest neighbour individuals start overlapping. This is obtained by considering that, by definition, $\langle \Delta r^2(\tau_o) \rangle^{1/2} = \frac{\lambda}{2}$ and that, on the length-scale λ, the diffusion is closely Fickian-like, $\langle \Delta r^2(\tau_o) \rangle = (6 D_L \tau_o)$, which results in the relation $(6 D_L \tau_o)^{1/2} = \frac{\lambda}{2}$. By doing so, we obtain $\tau_o = \frac{\lambda^2}{24 D_L} \simeq 3.5$ s. This time can be interpreted as a very lower boundary for the waiting time needed for and individual to meet one of its neighbours. Overall,

the just discussed computations demonstrate that an homogeneous spatial distribution ensures negligible interactions among individuals and, in turn, poor crowding effects over the whole range of investigated densities.

4.2 Behavioural adaptations in *C. typicus* motion

The occurrence of the mixed ballistic-diffusive motion in the MSD behaviour is emerging as a quite universal property in swimming zooplankton [35], as also recently reported for a different calanoid species, *Clausocalanus furcatus* [28]. The characteristic time and length scales for *C. furcatus* are also strikingly similar to those recorded for *C. typicus*, pointing to possible evolutionary mechanisms in copepod movement.

The ballistic-to-diffusive crossover in the MSD seems to be a quite universal property in swimming zooplankton, as reported for other species [28, 35] but the shape of this crossover may be species-dependent: smooth in *C. typicus* and along a plateau in *C. furcatus*, at least in similar prey-rich environmental conditions. This difference is likely attributable to the swimming behaviour of the two copepods. *C. typicus* is a cruise swimmer, moving continuously and smoothly in the fluid [49]. The smooth transition here shown is compliant with that reported for *C. typicus* nauplii [35], for adult *Temora longicornis* [35] and *Acartia tonsa* [43]. On the other hand, *C. furcatus* has a unique motion pattern with repetitive looping [34, 50] developing over scales compatible with the plateau in the MSD. The results of the present investigation thus confirm the ability of MSD function to discriminate distinct behaviour and point to species-specific (and consequently motion-specific) emergent properties.

As concerns the displacement distributions, we notice that the observed presence of exponential tails is an intriguing feature. It has been previously reported for a variety of material and biological systems and is typically as-

cribed to spatial correlations among different trajectories or to a distribution of single particle/organism diffusion coefficients [1, 51–53]. Testing whether similar mechanisms were at play also in the present experiments is an interesting problem that calls for further investigation.

Fractal dimension has been used to characterise the swimming motion of several copepod species and has proved to be a robust descriptor of track convolution [50, 54]. It is important to underline that the adoption of a fractal approach has sometimes been criticised [55, 56], some works from the literature lacking the necessary formal robustness and preliminary verification of the applicability of fractal framework. In the present work, we have verified the self-similar signature, which is maintained over three to four orders of magnitude, thus guaranteeing the safe applicability of this descriptor. The estimation of D_{3D} reveals the maintenance of the same level of track convolution independent of the crowding, while the parallel calculation of D_{xy}, D_{xz} and D_{yz} points to an isotropic motion, without any directional preference. Numerical simulations [57–59] reveal the close relationship between D_{3D} and the encounter probability with prey, predators and mates. As such, a given D_{3D} represents a behavioural trade off between maximisation of ”positive” encounters (with prey and mates) and minimisation of ”negative” ones (with predators). The description of tracks with statistically similar degree of convolution (both in 3D and in 2D) suggests that the motion of *C. typicus* is optimised also in terms of potential disturbing effects due to crowding, and that the level of convolution set by the tracks represents a dynamic adaptation to a variable environment. The results here presented also confirm the impossibility of retrieving 3D information from 2D projections, as previously indicated by [29] and [16]. This latter evidence supports the adoption of specifically 3D computational tools to evaluate the full degree of convolution of space-occupying tracks. Overall, the fractal characterisation carried out in the present study backs up the suitabil-

ity of this descriptor as a non-invasive assessment of the health of copepods [44]. The same approach has been used to check for any anisotropy in the two-dimensional motion of *C. typicus*. For each crowding condition, the D_{xy}, D_{xz} and D_{yz} of a given sex are always statistically similar (Kruskal-Wallis analysis of variance $p > 0.01$). This indicates that both females and males move isotropically in their environment, and consequently their motion does not display any directional preference but the same degree of convolution is maintained over the three Cartesian planes.

In [31] the average squared velocity was used as a measure for the activity level in a population of the freshwater cladoceran *Daphnia pulicaria* infected by *Vibrio cholerae*. The infected *D. pulicaria* showed a considerably higher level of activity (or, equivalently, higher ecological temperature), which would make them more easily detectable to predators such as fish [60], verifying the suitability of the descriptor to highlight behavioural differences. In the present study, we apply for the first time the ecological temperature to trajectories described by a marine copepod, extending the range of applications of this metric. The results indicate that the average ecological temperature does not show a clear trend on crowding for *C. typicus*, and is overall compatible with a constant value within the statistical uncertainty. Hence, the outcomes of ecological temperature do support the aforementioned picture of an homeostatic mechanism at play.

4.3 Adapting to crowding - Ecological implications

The results gathered in this study specifically refer to *Centropages typicus*, and consequently cannot be automatically generalised, as species-specific responses may differ. Nonetheless, it might be realistic to expect that similar levels of crowding in other pelagic calanoids of similar size and cruising behaviour

(*e.g.*, *Pseudocalanus elongatus*, *Euritemora affinis*, *Temora stylifera* and *Temora longicornis*; [61]) may lead to similar results. The experiments presented here were run over short-time windows, therefore the behaviour recorded must be considered as an immediate adaptation of *C. typicus* to an acute stress. Future efforts will be devoted to the investigation of any time-dependent behavioural acclimation, as done in [43]. It should also be considered that the highest crowding levels used in this study correspond to the lower end range of abundances often tested in the literature on other species, *e.g. Acartia steueri* [15], *A. tonsa* [19, 43, 62], and *E. affinis* [63]. Future investigations will therefore need to include also crowding levels above the ones here tested.

The integrative approach applied in this study supports building a more complete description of the swimming performance of *C. typicus*, thus gaining a comprehensive picture of any potential effect of crowding on their swimming fitness. It is worth underlining that, over similar ranges of densities, also the calanoid copepod *Eurytemora affinis* did not show significant variations in movement descriptors [16]. At even much higher values (up to 80 ind. mL^{-1}), the cyclopoid *Oithona davisae* showed metabolic rates in proportion to the temperature although the motor activity parameters were unaffected by short-term crowding [64, 65]. The density levels adopted in the present experiments could consequently be used in observational and behavioural studies or in rearing conditions without expected consequences on animal health or motion patterns.

The time span of the experiments also allowed excluding any relevant oxygen depletion in the setup. Considering an indicative oxygen consumption rate of 0.157 μL O_2 h $^{-1}$ cop $^{-1}$ for *C. typicus* [66], at the highest copepod density used in our tests (100 ind. L^{-1}) undersaturation might be critical after several hours. Running short-time experiments thus excludes that the behaviour observed might have been influenced by hypoxia.

The maintenance of similar values for all the descriptors used in this work, independently of the crowding condition tested, suggests an overall optimality in the swimming performance of *C. typicus*. Even at the highest density tested, none of the descriptors used showed significant variations. This indicates that, over the range of crowding tested, the typical distance between the individuals is always large enough to determine appreciable changes in the descriptors. Such an evidence can be explained considering the distance between individuals. Assuming a perceptive radius of 1 mm centred on *C. typicus* body, each individual would have a perceptive volume of 4.19 mm^3. An interaction between two organisms would be effective only when their perceptive volumes would overlap. At the highest density tested, however, the total volume occupied by the individual would represent less than the 0.1% of that of the experimental aquarium (1 L). Such a small ratio ensures that encounters are rare, provided that the spatial distribution is homogeneous (no clustering), as suggested in Sec. 4.1. Individual behaviour can be modulated by triggers acting at different scales [40]. When both organisms involved in the interaction are moving, the shape of the encounter zone may impact the effective encounter rate [89]. The assumption of a spherical encounter zone for *C. typicus*, however, can be considered a valid oversimplification at least in the framework of the process-oriented model here outlined.

Fine-scale movement details may not only impact the overall fitness of single organisms, but their consequences may also scale up to population, community and ecosystem levels [40, 41]. Individual behaviour can respond differently, with different outcomes at community level [67], but it can also impact on the environment itself [68]. Based on this evidences, it is important to pay attention to variations in individual movement, and include such details in predictive models to properly interpret ecological dynamics [40]. Along this line, the study here presented underlines the critical need to resolve individual-scale

behaviour in copepods to aptly understand the functioning of pelagic ecosystems under different conditions.

5. ACKNOWLEDGMENTS

The experiments were performed in the framework of GB's PhD thesis supported by the Stazione Zoologica Anton Dohrn. MU's visit to the University of Wisconsin - Milwaukee in January 2017 was supported by the Simons Foundation grant "Collaboration on Mathematical Biology" (Award # 278436) to PH. This work was financially supported by Stazione Zoologica Anton Dohrn PhD program and internal grant funds, and by Simons Foundation grant "Collaboration on Mathematical Biology" (Award # 278436). The funding agencies had no role in study design, data collection and analysis, decision to publish, or preparation of the manuscript. The authors thank two anonymous reviewers for valuable comments on the manuscript.

---

[1] Weeks ER, Crocker JC, Levitt AC, Schofield A, Weitz DA. Three-dimensional direct imaging of structural relaxation near the colloidal glass transition. Science. 2000;287:627–631.

[2] Bechinger C, Di Leonardo R, Löwen H, Reichhardt C, Volpe G, Volpe G. Active particles in complex and crowded environments. Reviews of Modern Physics. 2016;88:045006.

[3] Kabla AJ. Collective cell migration: leadership, invasion and segregation. Journal of The Royal Society Interface. 2012;9(77):3268–3278.

[4] Gravish N, Gold G, Zangwill A, Goodisman MA, Goldman DI. Glass-like dynamics in confined and congested ant traffic. Soft Matter. 2015;11:6552–6561.

[5] Cavagna A, Cimarelli A, Giardina I, Parisi G, Santagati R, Stefanini F, et al. Scale-free correlations in starling flocks. Proceedings of the National Academy of Sciences. 2010;107(26):11865–11870.

[6] Lopez U, Gautrais J, Couzin ID, Theraulaz G. From behavioural analyses to models of collective motion in fish schools. Interface Focus. 2012;2(6):693–707.

[7] Huys R, Boxshall G. Copepod Evolution. London: The Ray Society; 1991.

[8] Uttieri M. Trends in copepod studies. In: Uttieri M, editor. Trends in Copepod Studies - Distribution, Biology and Ecology. New York: Nova Science Publishers; 2018. p. 1–11.

[9] Byron E, Whitman P, Goldman C. Observations of copepod swarms in Lake Tahoe. Limnology and Oceanography. 1983;28:378–382.

[10] Ueda H, Kuwahara A, Tanaka M, Azeta M. Underwater observations on copepod swarms in temperate and subtropical waters. Marine Ecology Progress Series. 1983;11:165–171.

[11] Buskey EJ, Peterson JO, Ambler JW. The swarming behavior of the copepod *Dioithona oculata*: In situ and laboratory studies. Limnology and Oceanography. 1996;41:513–521.

[12] Raisuddin S, Kwok KWH, Leung KMY, Schlenk D, Lee JS. The copepod *Tigriopus*: A promising marine model organism for ecotoxicology and environmental

genomics. Aquatic Toxicology. 2007;83:161–173.

[13] Carotenuto Y, Esposito F, Pisano F, Lauritano C, Perna M, Miralto A, et al. Multi-generation cultivation of the copepod *Calanus helgolandicus* in a re-circulating system. Journal of Experimental Marine Biology and Ecology. 2012;418-419:46–58.

[14] Hansen BW. Advances using Copepods in Aquaculture. Journal of Plankton Research. 2017;39:972–974.

[15] Takayama Y, Hirahara M, Liu X, Ban S, Toda T. Are egg production and respiration of the marine pelagic copepod Acartia steueri influenced by crowding? Aquaculture Research. 2020;51(9):3741–3750.

[16] Dur G, Souissi S, Schmitt F, Michalec FG, Mahjoub MS, Hwang JS. Effects of animal density, volume, and the use of 2D/3D recording on behavioral studies of copepods. Hydrobiologia. 2011;666:197–214.

[17] Miralto A, Ianora A, Poulet SA, Romano G, Laabir M. Is fecundity modified by crowding in the copepod *Centropages typicus*? Journal of Plankton Research. 1996;18:1033–1040.

[18] Drillet G, Rais M, Novac A, Jepsen PM, Mahjoub MS, Hansen BW. Total egg harvest by the calanoid copepod *Acartia tonsa* (Dana) in intensive culture – effects of high stocking densities on daily egg harvest and egg quality. Aquaculture Research. 2015;46:3028–3039.

[19] Vu MTT, Hansen BW, Kiørboe T. The constraints of high density production of the calanoid copepod *Acartia tonsa* Dana. Journal of Plankton Research. 2017;39:1028–

1039.

[20] Jepsen PM, Andersen CVB, Schjelde J, Hansen BW. Tolerance of un-ionized ammonia in live feed cultures of the calanoid copepod *Acartia tonsa* Dana. Aquaculture Research. 2015;46:420–431.

[21] Uttieri M, Nihongi A, Hinow P, Motschman J, Jiang H, Alcaraz M, et al. Copepod manipulation of oil droplet size distribution. Scientific Reports. 2019;9:547.

[22] Razouls C, de Bovée F, Kouwenberg J, Desreumaux N. Diversity and geographic distribution of marine planktonic copepods; 2005-2020. Accessed: 2020-06-07. http://copepodes.obs-banyuls.fr/en.

[23] Mauchline J. The Biology of Calanoid Copepods. vol. 33 of Advances in Marine Biology. London: Academic Press; 1998.

[24] Carlotti F, Harris R. The biology and ecology of *Centropages typicus*: An introduction. Progress in Oceanography. 2007;72:117–120.

[25] Price HJ, Paffenhöfer GA, Boyd CM, Cowles TJ, Donaghay PL, Hamner WM, et al. Future studies of zooplankton behavior: questions and technological developments. Bulletin of Marine Science. 1988;43(3):853–872.

[26] Sabia L, Uttieri M, Schmitt FG, Zagami G, Zambianchi E, Souissi S. *Pseudodiaptomus marinus* Sato, 1913, a new invasive copepod in Lake Faro (Sicily): observations on the swimming behaviour and the sex-dependent responses to food. Zoological Studies. 2014;53:49.

[27] Seuront L. When complexity rimes with sanity: loss of fractal and multifractal behavioural complexity as an indicator of sublethal contaminations in zooplankton. In: Ceccaldi HJ, Hénocque Y, Koike Y, Komatsu T, Stora G, Tusseau-Vuillemin MH, editors. Marine Productivity: Perturbations and Resilience of Socio-ecosystems. New York: Springer Verlag; 2015. p. 129–137.

[28] Pastore R, Uttieri M, Bianco G, Ribera d'Alcalá M, Mazzocchi M. Distinctive diffusive properties of swimming planktonic copepods in different environmental conditions. European Physical Journal E. 2018;41:79.

[29] Uttieri M, Zambianchi E, Strickler JR, Mazzocchi MG. Fractal characterization of three-dimensional zooplankton swimming trajectories. Ecological Modelling. 2005;185:51–63.

[30] Uttieri M, Zambianchi E. On the fractal characterisation of zooplankton motion: applications and perspectives. In: Mitchell EW, Murray SR, editors. Classification and Application of Fractals: New Research. New York: Nova Science Publishers; 2012. p. 113–129.

[31] Hinow P, Nihongi A, Strickler JR. Statistical mechanics of zooplankton. PLoS One. 2015;8:e0135258.

[32] Mazzocchi MG, Dubroca L, García-Comas C, Di Capua I, Ribera d'Alcalá M. Stability and resilience in coastal copepod assemblages: The case of the Mediterranean long-term ecological research at Station MC (LTER-MC). Progress in Oceanography. 2012;97-100:135–151.

[33] Di Capua I, Mazzocchi MG. Population structure of the copepods *Centropages typicus* and *Temora stylifera* in different environmental conditions. ICES Journal of Marine Science. 2004;61:632–644.

[34] Bianco G, Botte V, Dubroca L, Ribera d'Alcalá M, Mazzocchi MG. Unexpected regularity in swimming behavior of *Clausocalanus furcatus* revealed by a telecentric 3D computer vision system. PLoS One. 2013;8:e67640.

[35] Visser AW, Kiørboe T. Plankton motility patterns and encounter rates. Oecologia. 2006;148:538–546.

[36] Meroz Y, Sokolov IM. A toolbox for determining subdiffusive mechanisms. Physical Reports. 2015;573:1–29.

[37] Margalef R. Perspectives in Ecological Theory. Chicago: University of Chicago Press; 1968.

[38] Kiørboe T, Bagøien E. Motility patterns and mate encounter rates in planktonic copepods. Limnology and Oceanography. 2005;50(6):1999–2007.

[39] Jeltsch F, Grimm V. Editorial: thematic series "Integrating movement ecology with biodiversity research". Movement Ecology. 2020;8:19.

[40] Shaw AK. Causes and consequences of individual variation in animal movement. Movement Ecology. 2020;8:12.

[41] Tyson RC. The princess and the pea: the unexpected importance of movement algorithms. In: Mondaini RP, editor. BIOMAT 2013 - Proceedings of the International Symposium on Mathematical and Computational Biology. Singapore:

World Scientific; 2013. p. 1–27.

[42] Turchin P. Quantitative Analysis of Movement. Sunderland: Sinauer Press; 1998.

[43] Nilsson B, Jakobsen HH, Stief P, Drillet G, Hansen BW. Copepod swimming behavior, respiration, and expression of stress-related genes in response to high stocking densities. Aquaculture Reports. 2017;6:35–42.

[44] Seuront L. Behavioral fractality in marine copepods: endogenous rhythms versus exogenous stressors. Physica A. 2011;390:250–256.

[45] Markovic D, Gros C. Self-organized chaos through polyhomeostatic optimization. Physical Review Letters. 2010;105(6):068702.

[46] Turrigiano GG, Nelson SB. Homeostatic plasticity in the developing nervous system. Nature Reviews Neuroscience. 2004;5(2):97–107.

[47] Vargas P, Moioli R, de Castro LN, Timmis J, Neal M, Von Zuben FJ. Artificial homeostatic system: a novel approach. In: Capcarrère MS, Freitas AA, Bentley PJ, Johnson CG, Timmis J, editors. European Conference on Artificial Life. vol. 3630 of Lecture Notes in Computer Science. Springer; 2005. p. 754–764.

[48] Butz M, Steenbuck ID, van Ooyen A. Homeostatic structural plasticity increases the efficiency of small-world networks. Frontiers in Synaptic Neuroscience. 2014;6:7.

[49] Alcaraz M, Saiz E, Calbet A. Centropages behaviour: swimming and vertical migration. Progress in Oceanography. 2007;72(2):121–136.

[50] Uttieri M, Paffenhöfer GA, Mazzocchi MG. Prey capture in *Clausocalanus furcatus* (Copepoda: Calanoida). The role of swimming behaviour. Marine Biology. 2008;153:925–935.

[51] Wang B, Kuo J, Bae SC, Granick S. When Brownian diffusion is not Gaussian. Nature Materials. 2012;11:481–485.

[52] Hapca S, Crawford JW, Young IM. Anomalous diffusion of heterogeneous populations characterized by normal diffusion at the individual level. Journal of the Royal Society Interface. 2009;6(30):111–122.

[53] Pastore R, Ciarlo A, Pesce G, Greco F, Sasso A. Rapid Fickian Yet Non-Gaussian Diffusion after Subdiffusion. Physical Review Letters. 2021;126(15):158003.

[54] Uttieri M, Nihongi A, Mazzocchi MG, Strickler JR, Zambianchi E. Pre-copulatory swimming behaviour of *Leptodiaptomus ashlandi* (Copepoda: Calanoida): a fractal approach. Journal of Plankton Research. 2007;29:i17–i26.

[55] Turchin P. Fractal analyses of animal movement: a critique. Ecology. 1996;77:2086–2090.

[56] Halley JM, Hartley S, Kallimanis AS, Kunin WE, Lennon JJ, Sgardelis SP. Uses and abuses of fractal methodology in ecology. Ecology Letters. 2004;7:254–271.

[57] Uttieri M, Cianelli D, Strickler JR, Zambianchi E. On the relationship between fractal dimension and encounters in three-dimensional trajectories. Journal of Theoretical Biology. 2007;247(3):480– 491.

[58] Cianelli D, Uttieri M, Strickler JR, Zambianchi E. Zooplankton encounters in patchy particle distributions. Ecological Modelling. 2009;220(5):596–604.

[59] Uttieri M, Cianelli D, Zambianchi E. Behaviour-dependent predation risk in swimming zooplankters. Zoological Studies. 2013;52:32.

[60] Nihongi A, Ziarek JJ, Nagai T, Uttieri M, Zambianchi E, Strickler JR. *Daphnia pulicaria* hijacked by *Vibrio cholera*: Altered swimming behavior and predation risk implications. In: Kattel G, editor. Zooplankton and Phytoplankton. Nova Science Publishers; 2011. p. 181–192.

[61] Svetlichny L, Larsen PS, Kiørboe T. Kinematic and dynamic scaling of copepod swimming. Fluids. 2020;5(2):68.

[62] Franco SC, Augustin CB, Geffen AJ, Dinis MT. Growth, egg production and hatching success of *Acartia tonsa* cultured at high densities. Aquaculture. 2017;468:569–578.

[63] Ban S, Minoda T. Induction of diapause egg production in *Eurytemora affinis* by their own metabolites. Hydrobiologia. 1994;292/293:185–189.

[64] Svetlichny L, Hubareva E, Khanaychenko A, Gubanova A, Altukhov D, Besiktepe S. Adaptive strategy of thermophilic *Oithona davisae* in the cold Black Sea environment. Turkish Journal of Fisheries and Aquatic Sciences. 2016;16(1):77–90.

[65] Svetlichny L, Hubareva E, Uttieri M. Ecophysiological and behavioural responses to salinity and temperature stress in cyclopoid copepod *Oithona davisae* with comments on gender differences. Mediterranean Marine Science. 2021;22(1):89–101.

[66] Raymont JEG. The respiration of some planktonic copepods. Limnology and Oceanography. 1959;4:479–491.

[67] Gordon DM. The fusion of behavioral ecology and ecology. Behavioral Ecology. 2011 03;22(2):225–230.

[68] López-Sepulcre A. The many ecologies of behavior. Behavioral Ecology. 2011 03;22(2):232–233.